A new species of Girdled Lizard (Squamata: Cordylidae) from the Serra da Neve Inselberg, Namibe Province, southwestern Angola

6 authors, including:

Article

A new species of Girdled Lizard (Squamata: Cordylidae) from the Serra da Neve Inselberg, Namibe Province, southwestern Angola

MARIANA P. MARQUES[1,2,7], LUIS M. P. CERÍACO[3,2], EDWARD L. STANLEY[4], SUZANA A. BANDEIRA[5,6], ISHAN AGARWAL[5] & AARON M. BAUER[5]

[1]*Research Center in Biodiversity and Genetic Resources (CIBIO), Research Network in Biodiversity and Evolutionary Biology (InBIO), University of Porto, Rua Padre Armando Quintas 7, Vairão, 4485-661 Porto, Portugal*
[2]*Departamento de Zoologia e Antropologia (Museu Bocage), Museu Nacional de História Natural e da Ciência, Universidade de Lisboa, Rua da Escola Politécnica, 58, 1269-102 Lisboa, Portugal*
[3]*Museu de História Natural e da Ciência da Universidade do Porto, Praça Gomes Teixeira 4099-002 Porto, Portugal*
[4]*Department of Natural History, Florida Museum of Natural History, University of 17 Florida, Gainesville, Florida 32611, USA*
[5]*Department of Biology, Villanova University, 800 Lancaster Avenue, Villanova, Pennsylvania 19085-1699, USA*
[6]*Instituto Nacional da Biodiversidade e Áreas de Conservação, Ministério do Ambiente de Angola, Centralidade do Kilamba, Rua 26 de Fevereiro, Quarteirão Nimi Ya Lukemi, edifício Q11, 3° andar, Luanda, Angola.*
[7]*Corresponding author. E-mail: mptlmarques@gmail.com*

Abstract

A new species of rupicolous girdled lizard is described from Serra da Neve Inselberg, Namibe Province, southwestern Angola. We sequenced two mitochondrial gene regions (16S and ND2) for the new species and compared these data with those previously published for other *Cordylus* species. The new species is genetically divergent from the closely related *Cordylus machadoi* and *C. namakuiyus* and morphologically distinguished by head scale arrangement, coloration, and osteological characters. Serra da Neve is the second highest peak in Angola and one of the most understudied areas of the country. The discovery of this new species highlights the importance of this inselberg for regional endemism and emphasizes the high conservation importance of the area.

Key words: *Cordylus phonolithos* **sp. nov.**, molecular phylogeny, computed tomography, endemism, taxonomy, Africa

Resumo

Uma nova espécie de lagarto-espinhoso-rupícola é descrita do Inselberg da Serra da Neve, situado na província do Namibe, sudoeste de Angola. Foram sequenciados dois genes mitocondriais (16S e ND2) da nova espécie, que foram subsequentemente comparados com os dados anteriormente publicados para outras espécies do género *Cordylus*. A nova espécie é geneticamente divergente das espécies congéneres, *Cordylus machadoi* e *C. namakuiyus*, e morfologicamente pode-se distinguir pelo arranjo das escamas cefálicas, coloração e por caracteres osteológicos. A Serra da Neve é o segundo pico mais alto de Angola e uma das áreas menos estudadas do país. A descoberta desta nova espécie destaca a importância deste Inselberg e enfatiza a importância de conservar esta área.

Palavras chave: *Cordylus phonolithos* **sp. nov.**, filogenia molecular, tomografia computorizada, endemismo, taxonomia, África

Introduction

The genus *Cordylus* Laurenti, 1768, comprises 22 currently recognized species of diurnal rupicolous lizards, endemic to sub-Saharan Africa (Poynton & Broadley 1978; Branch 1998; Branch *et al.* 2005; Stanley *et al.* 2011; Nielsen & Colston 2014; Uetz *et al.* 2019). Recent phylogenetic studies by Stanley *et al.* (2011, 2016) have revealed that *Cordylus* is divided into two disjunct lineages: a southern clade, comprising a total of nine species restricted to

the southwestern quadrant of South Africa, and a northern clade comprising 13 species distributed along the eastern escarpment from South Africa to Ethiopia, of which three species occur from central and southwestern Angola to northwestern Namibia. The taxonomic diversity of the northern clade has increased significantly in the past 20 years with the description of *C. nyikae* Broadley & Mouton, 2000, *C. beraduccii* Broadley & Branch, 2002, *C. meculae* Branch, Rödel & Marais, 2005, *C. marunguensis* Greenbaum, Stanley, Kusamba, Moninga, Goldberg & Bursey, 2012, and *C. namakuiyus* Stanley, Ceríaco, Bandeira, Valério, Bates & Branch, 2016.

Regarding the three Angolan and Namibian species, the Angolan girdled lizard, *C. angolensis* (Bocage, 1895) is endemic to the central escarpment of Angola, (Kwanza Sul and Huíla Provinces), the Kaokoveld Girdled Lizard, *C. namakuiyus*, is endemic to the arid lowlands of Namibe desert and subdesert of southwestern Angola, and Machado's Girdled Lizard, *C. machadoi* Laurent, 1964, is restricted to the southwestern Angolan escarpment and high plateaus of Huíla Province (Marques *et al.* 2018). In Namibia, the genus has been reported from the Baynes and Otjipha Mountains in the Kunene Region in the northwestern regions of the country (Branch 1998; Stanley *et al.* 2016), though the specific identity of these specimens remains unknown.

The herpetofauna of Southwestern Angola is the most well-studied of the country, representing approximately one third of the total number of species-level taxa known to occur in the country (Ceríaco *et al.* 2016; Baptista *et al.* 2018; Marques *et al.* 2018; Butler *et al.* 2019). In recent years, southwestern Angola has received special attention from several research teams, with herpetological surveys conducted in Namibe Province (e.g., Conradie *et al.* 2012; Ceríaco *et al.* 2016). Several new species of amphibians and reptiles have been described based on the results of these surveys, including the Serra da Neve Pygmy Frog, *Poyntonophrynus pachnodes* Ceríaco, Marques, Bandeira, Agarwal, Stanley, Bauer, Heinicke & Blackburn, 2018, the Kaokoveld Girdled Lizard, *C. namakuiyus*, Haacke's Sand Lizard, *Pedioplanis haackei* Conradie, Measey, Branch & Tolley, 2012, and Huntley's Sand Lizard, *P. huntleyi* Conradie, Measey, Branch & Tolley, 2012. Other species of reptiles are currently in the process of being described. Namibe Province is an important area as it encompasses two important biogeographic zones—the "true desert zone" forms a strip of dune desert in southwestern Namibe Province, extending northward from the Skeleton Coast of Namibia, and a low elevation "semidesert" zone characterized by xeric vegetation, that extends from southern Benguela, to the Kaokoveld of Namibia (Marques *et al.* 2018). These two zones host a spectacular diversity of reptiles, many of them endemic or near-endemic (Marques *et al.* 2018).

The landscape of southwestern Angola is characterized by the presence of isolated mountain-like rocky outcrops of subvolcanic origin mostly composed of gneisses, migmatites and granites (Pereira & Moreira 1977). Due to microclimatic conditions and habitats that differ from the surrounding lowlands, these inselbergs support unique biological communities and high levels of endemism (Simons *et al.* 1998; Porembski & Barthlott 2000; Porembski *et al.* 2000; Bruke 2001, 2003, 2005; Porembski 2007; Michael *et al.* 2008; Brand *et al.* 2011; Bayliss *et al.* 2014). In recent years several new endemic species, such as amphibians (Ceríaco *et al.* 2018; Conradie *et al.* 2018), reptiles (Branch *et al.* 2005; Branch & Bayliss 2009; Branch & Tolley 2010; Portik *et al.* 2013; Branch *et al.* 2014), invertebrates (Congdon *et al.* 2010; Daniels & Bayliss 2012; Bilton 2014; Daniels *et al.* 2014), and mammals (Monadjem *et al.* 2010; Taylor *et al.* 2012) have been described from inselbergs across Africa. The Serra da Neve complex (Fig. 1) is an inselberg with a basal area of approximately 630 km², located at the northern limit of Namibe Province, southwestern Angola. Serra da Neve is the second highest peak of Angola, with an elevation of 2489 m (Pereira 1977), and is covered by a sparse "Miombo" forest habitat (Grandvaux-Barbosa 1970), contrasting with the surrounding lowland habitats, mainly dominated by Namibian woodland savanna, and arid areas of Namib Desert (Grandvaux-Barbosa 1970). Despite its prominence in the southwestern Angolan landscape, Serra da Neve remains very poorly explored.

During recent field research in southwestern Angola, which included Serra da Neve and its surrounding lowland areas, as well as the southwestern escarpment of Namibe/Huíla provinces, we collected two species of *Cordylus*. These include new records of *C. machadoi* from the Tundavala area, Huíla Province (Butler *et al.* 2019), and specimens of a putatively new species in N'Dolondolo area, at the base of Serra da Neve. While morphologically intermediate between *C. machadoi* and *C. namakuiyus*, the newly collected specimens present some morphological characters that differentiate it from all other Angolan species. These differences are also supported by molecular phylogenetic data. Based on these data we conclude that the N'Dolondolo population represents an undescribed taxon. We place the description of this new species in the context of current knowledge regarding Serra da Neve biogeography and southwestern African inselbergs.

FIGURE 1. Southern slopes of Serra da Neve, southwestern Angola (Photo by Luis Ceríaco).

Material and methods

Two new specimens of the putative new species of *Cordylus* sp. from N'Dolondolo (Namibe Province, Angola) were collected for this study (CAS 263581, INBAC/AMB 10272—see details in the Systematics section and Appendix I). The specimens collected for this study were euthanized following an approved IACUC protocol (Villanova University #1866), preserved in 10% buffered formalin in the field and transferred to 70% ethanol for storage at the conclusion of the expedition. Liver tissue was removed before formalin fixation and preserved in RNALater and transferred to 95% ethanol for storage. Specimens were deposited in both the California Academy of Sciences (CAS; San Francisco, USA), and in the Instituto Nacional da Biodiversidade e Áreas de Conservação (INBAC; Kilamba-Kiaxi, Angola). Relevant specimens deposited in the collections of the American Museum of Natural History (AMNH; New York, USA) and Museu Regional do Dundo (MD; Dundo, Angola) were also consulted for comparisons (see Appendix I; Fig. 2), as were mensural and meristic data of other *Cordylus* species retrieved from relevant literature (Loveridge 1944; Branch 1998; Broadley & Branch 2002; Greenbaum *et al.* 2012; Stanley *et al.* 2016).

    Morphological methods. External morphological analyses followed the procedures of Broadley & Branch (2002), Greenbaum *et al.* (2012) and Stanley *et al.* (2016). We recorded morphometric data from preserved specimens, using digital calipers (0.1 mm) under a stereo-microscope. Measurements were collected by the first author (MPM) on the right side of each specimen, or on the left side if the specimen was damaged: snout–vent length (SVL), measured from the tip of snout to anterior margin of vent; tail length (TL), from the posterior margin of vent to tail tip, measured only on specimens with complete and original tails; head length (HL), measured from the tip of snout to posterior margin of temporals; maximum head width (HW), measured at the broadest part; head height (HH), measured at midpoint of eye from top of head to bottom of lower jaw; snout–eye length (SEL), from the tip of snout to the anterior margin of eye; snout–arm length (SAL), measured from the tip of snout to anterior margin of the forelimb; axilla-groin distance (AGD), from the posterior edge of forelimb insertion to the anterior edge of hind limb insertion; humerus length (HML); radius-ulna length (RUL); femur length (FL); tibia-fibula length

(TFL); longest toe length (LTL), length of fourth toe on hind limb. Meristic data were also collected on the right side of each specimen, or on the left side if the specimen was damaged, except for femoral pore and generation gland counts if field/museum tags obscured the right thigh. Scale counts included: femoral pores (FP); generation glands (GEN); chin shields (CS); supralabials (SL), all scales bordering upper lip, except rostral, to posterior border of eye; infralabials (IL), all scales bordering lower lip, except mental, to large posterior labial (included); supraoculars (SO); supraciliaries (SC); loreals (LO); subocculars (SOC), all scales bordering eye and in contact with the SLs with the exception of the anterior one (i.e. preocular); preoculars (PRE); transverse row of gulars between posterior chin shields,(TGU), excluding small granular scales on either side; dorsal transverse rows (DTR), from immediately behind occipital to base of tail above vent; dorsolateral longitudinal rows (DLLR), midway between fore- and hind limbs, excluding small scales in the lateral fold; ventral transverse rows (VTR), axilla to the groin; ventral longitudinal rows (VLR), midway between fore- and hind limbs, excluding small, often keeled, pseudo-ventrals on either side; caudal scales (CDS), counted around the tail at the position of the 11th and 15th scale to avoid possible differences between males (swollen tail base) and females; subdigital lamellae on fingers (SDF1 to SDF5) and toes (SDT1 to SDT5).

Osteological data were obtained from CAS 263581 (holotype of the new species described below) and comparative material using High Resolution X-ray Computed Tomography (HRCT). CAS 263581 was scanned using a Phoenix v|tome|x M at the University of Florida's Nanoscale Research Facility under the following conditions: 240 microXray tube settings =100 microamps, 200 kilovolts, 20 Watts, 4 x detector sensitivity, averaging three images taken at 200 millisecond intervals. Two separate scans were performed: one high resolution (voxel size 14.36μm) of the skull, and one lower resolution (voxel size 45.57μm) of the whole body. The resulting radiographs were converted to tomograms using the proprietary GE software Datos|x version 2.3. The resulting volumetric dataset and comparative material previously scanned for Stanley et al (2016) were processed, segmented and analyzed using VGStudioMax 3.2.4 (Volume Graphics, Heidelberg Germany). The skeleton and osteoderms were reconstructed separately for each scan to facilitate osteological analysis. The volume and thickness of osteoderms along the dorsal, ventral, caudal and limb areas were recorded for each of these scans. Tomograms and 3D mesh files are available for all comparative material on morphosource.org (see Supplementary Material 1).

Molecular methods. This study used the dataset used by Stanley *et al*. (2016), incorporating sequences of the mitochondrial 16S rRNA (591 bp) and ND2 (1176 bp) genes from the two Serra da Neve *Cordylus* specimens into a two gene dataset of 19 representative of *Cordylus* species and two outgroup taxa, *Ouroborus cataphractus* (Boie, 1828) and *Namazonurus campbelli* (FitzSimons, 1943). The original dataset is available on GenBank, and corresponding accession numbers are listed in Stanley *et al*. (2016). Novel sequences were generated from the two specimens collected in Serra da Neve for a partial fragment of 16S (CAS 263581: GENBANK # MN342159; AMB 10272: GENBANK # MN342160) and ND2 (CAS 263581: GENBANK # MN342161; AMB 10272: GENBANK # MN342162). All novel sequences were generated at Villanova University, Villanova (PA), USA using the following methods: total genomic DNA was extracted using a salt extraction protocol. Liver tissues were digested using a lysis solution of Proteinase K, 10% sodium dodecyl sulfate, and extraction buffer (1 M Tris, 5 M NaCl, 0.25 M EDTA, and distilled water). A 5 M NaCl solution was used to extract DNA and was subsequently washed with ethanol. Polymerase chain reaction (PCR) was used to amplify the mitochondrial genes, using the primers suggested by Stanley *et al*. (2016). PCR reactions were performed with a final volume of 22.5 μl containing: 9.9 μl sterile H_2O, 0.1 μl of *Taq* DNA polymerase (New England BioLabs, Ipswich, MA, USA), and 2.5 μl each of forward primer (8 ppm), reverse primer (8 ppm), 10x standard buffer (New England BioLabs), 5X-Q solution (Qiagen, Germantown, MD, USA), and dNTP mix. All PCR reactions were carried with an initial 2 min denaturation at 95˚C, followed by 32–34 cycles [35 s DNA denaturation at 95˚C, 35 s primer annealing at 50–52˚C, 1 min 35 s extension at 72˚C], and a final extension at 50˚C for 1 min. PCR products were tested for successful amplification using gel electrophoresis on 1.5% agarose gels. Successful PCR products were cleaned using magnetic bead protocols and sent to GENEWIZ (South Plainfield, NJ, USA) for sequencing on an ABI automated 3730xl genetic analyzer. Each of the 3′ to 5′ sequences were reverse-complemented and aligned with the corresponding 5′ to 3′ sequences and contiguous internal sequences using the program GeneiousTM v7.1 (Drummond *et al*. 2012), with the final sequence recovered from this consensus.

Phylogenetic analysis. Sequences were aligned using the MUSCLE alignment tool in MEGA X (Kumar *et al*. 2018). We performed phylogenetic analysis on the concatenated, partitioned, two gene datasets, with Maximum Likelihood (ML)—RAxML-HPC BlackBox 8.2.10 (Stamatakis 2006), and Bayesian inference (BI) optimality cri-

teria —MrBayes 3.2.6 (Ronquist *et al.* 2011) using the Cipres science gateway (Miller *et al.* 2010 -phylo.org). The dataset was partitioned by gene, and the most appropriate model of evolution for each locus identified using Akaike information criterion in MrModeltest v2.3 (Nylander 2008), resulting in identical models from those of Stanley *et al.* (2016; Table 1). Maximum Likelihood analyses of 16S and ND2 alignments were analyzed and data were carried out using with GTRCAT model sequence evolution. Phylogenetic robustness was estimated in the ML analyses by running 1000 random addition bootstrap replicates (Felsenstein 1985), while in the BI two separate Markov chains were run for 10 million generations, sampled every 1000 generations. We regarded tree topologies with bootstrap values of 70% or greater and posterior probabilities of over 0.95 as well-supported (Huelsenbeck & Hillis 1993). Pairwise comparisons of uncorrected sequence divergences (p-distance) were computed in MEGA X.
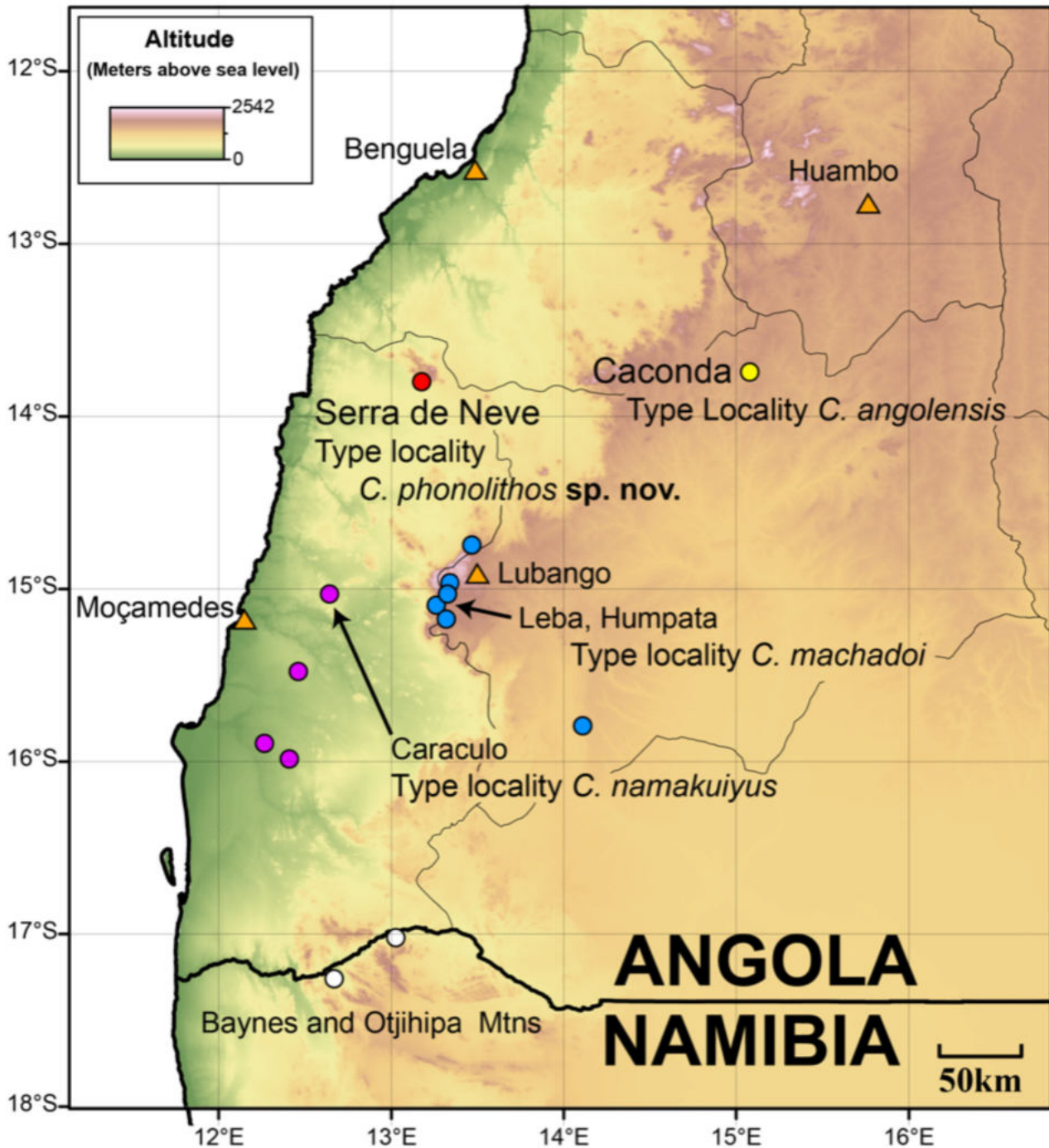
FIGURE 2. Map showing localities for *Cordylus* species in Angola. Yellow circle—*C. angolensis* (type locality: Caconda); Red circle—*C. phonolithos* **sp. nov,** (type locality: Serra da Neve); Blue circles—*C. machadoi* (type locality: Serra da Leba); Pink circles—*C. namakuiyus* (type locality: Caraculo). Major cities are represented by an orange triangle. Principal plotted localities include both bibliographic (Marques *et al.* 2018) and museum records.

Results

Molecular phylogenetic and morphological analyses suggest that the girdled lizards from N'Dolondolo represent an undescribed species of *Cordylus*. The 16S and ND2 trees were largely concordant. The phylogenetic analysis revealed that the N'Dolondolo population is a member of a strongly supported Angolan clade of *Cordylus*, phylogenetically sister to the two included Angolan taxa, although relationships among the three constituent taxa do not receive strong support (Fig. 3). The uncorrected pairwise distances between the new form and *C. machadoi* and *C. namakuiyus* for the mitochondrial marker ND2 averaged 7.3% and 6.7%, respectively (Table 1), and are consistent with interspecific differences in the genus *Cordylus* (Stanley *et al.* 2016), especially when regarding the average distance between the two other well-established Angolan species *C. machadoi* and *C. namakuiyus* (5.8%).
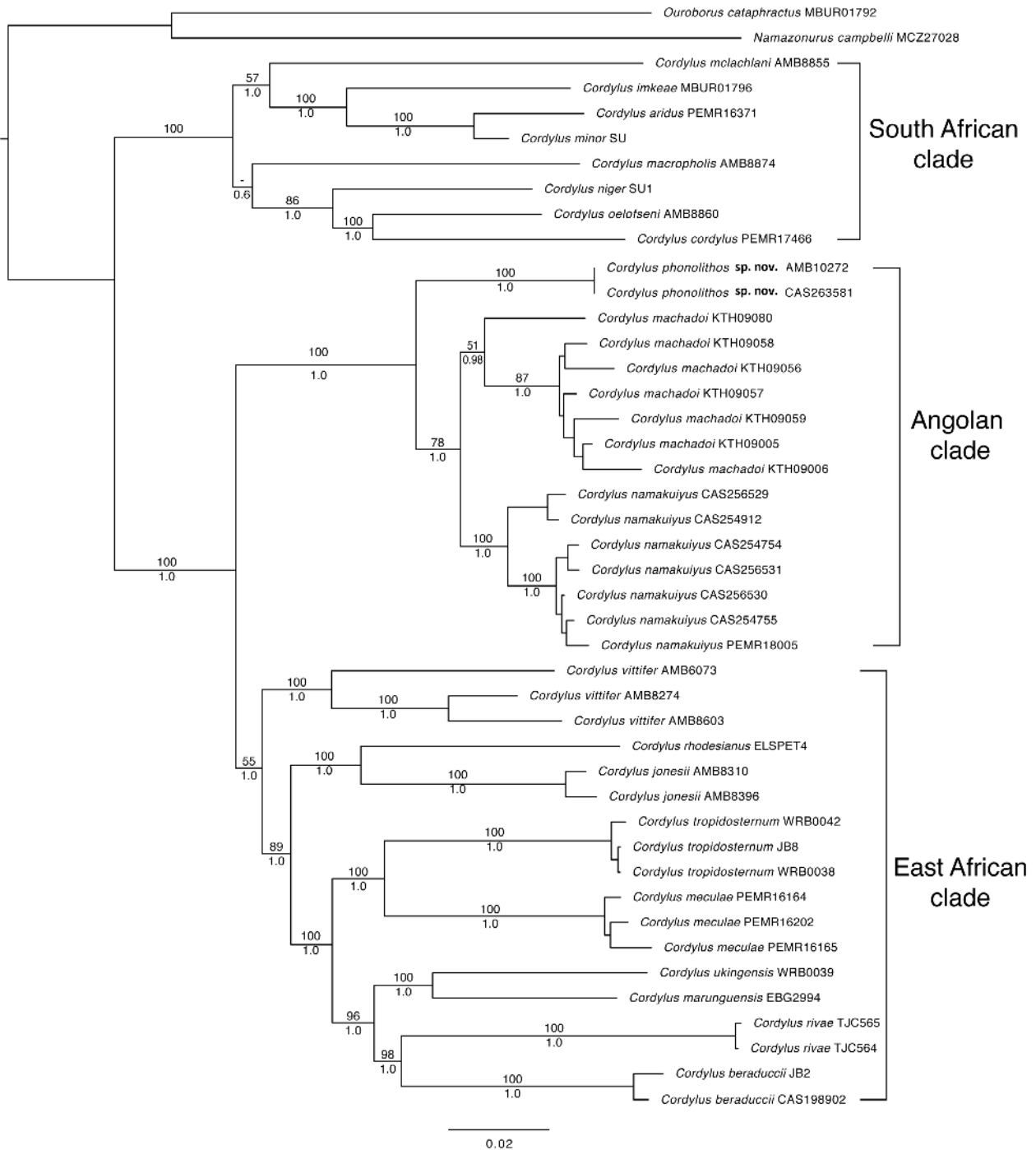
FIGURE 3. Maximum Likelihood tree for *Cordylus* based on ND2 with ML bootstraps above and BI posterior probabilities below.

Morphologically, the N'Dolondolo specimens are typical of *Cordylus* in having a robust but slightly flattened body; with well-developed limbs with unreduced digits, a triangular and flattened head covered with large shields; absence of occipital spines; lower eyelid well-developed without transparent window; dorsal transverse rows scales smooth to keeled; osteodermal armor underlying the scales of the head, limbs, dorsal and lateral trunk, and the spiny caudal scales (Branch 1998; Stanley *et al.* 2011). However, this population also exhibits a distinct combination of morphological characters that distinguish it from all described species of the genus in Angolan and surrounding countries, most notably the arrangement of head scales and a combination of several morphological and coloration characters (Table 2). Based on these differences and the genetic distinctiveness, this population is described here as a new species.

Systematics

Cordylus phonolithos sp. nov.
(Tables 1–2; Fig. 4–8)
lsid: urn:lsid:zoobank.org:act:813340B4-8299-4B1B-A786-5552BDC0C722

C. namakuiyus [part]: Stanley *et al.* (2016: 209)

Holotype. A subadult male (CAS 263581, field number AMB 10296; Figs. 4–5A) collected within a crevice in a granite boulder in the vicinity of N'Dolondolo (Figs. 2, 9), Namibe Province, Angola [-13.80678ºN, 13.13507ºE, 752 m elevation], collected by L. Ceríaco, S. Bandeira and I. Agarwal, on 21 November 2016.

FIGURE 4. Dorsal and ventral whole-body views (left) and Dorsal, lateral, and ventral views of the head of the holotype of *Cordylus phonolithos* **sp. nov.** (CAS 263581).

FIGURE 5. *Cordylus phonolithos* **sp. nov.** in life (**A.** Holotype CAS 263581; **B.** Paratype INBAC: AMB 10272). N'Dolondolo, Serra da Neve, southwestern Angola (Photos by Luis Ceríaco).

Paratype. A juvenile specimen (INBAC: AMB 10272 [same as field number]; Fig. 5B), collected at the same locality as the holotype, under a small granite rock on a larger rock, by the same collectors, on 20 November 2016.

Diagnosis. A medium sized *Cordylus* species, identified to genus by the following combination of characters: fully limbed, strongly depressed triangular head and body, osteoderms present, rhomboidal, imbricate and keeled dorsal scales present, occipitals non-spinose, and spinose caudal and limb scales enlarged (Branch 1998; Broadley & Branch 2002; Stanley *et al*. 2011). *Cordylus phonolithos* **sp. nov.** differs from all other species in the genus except

for *C. vittifer* (Reichenow, 1887)*, C. machadoi* and *C. namakuiyus,* by the presence (*versus* absence) of a transverse row of elongated dorsal scales immediately posterior to occipitals (Fig. 6). It is distinguished from *C. vittifer* by possessing an incomplete row of pre-occipital scales between posterior parietal and occipital scales (*versus* complete), and by having infralabials that are moderately deeply ridged (*versus* usually smooth). It is distinguished from *C. machadoi* by having a large keyhole-shaped interparietal in contact with frontoparietals and separating the anterior parietals (*versus* small, diamond-shaped interparietal not in contact with frontoparietal and never completely separating the anterior parietals in *C. machadoi*, see Fig. 6); having the intrusion of a scale in broad contact with the interparietal and occipitals, thereby separating posterior parietals (*versus* absence of this scale and posterior parietals in full contact in *C. machadoi*, see Fig. 6); a higher number of supralabials (6 in *C. phonolithos* **sp. nov.** *versus* 5 in *C. machadoi*); males with fewer caudal scales at the 15th tail whorl (8 in *C. phonolithos* **sp. nov.** *versus* 10–11 in *C. machadoi*); an orange-brown dorsal body coloration (*versus* darker brown to black in *C. machadoi*), the absence of dark speckles on throat and ventral body surfaces (*versus* presence in *C. machadoi*) and a reduced, widely separated posteromedial parietal process (similar to *C. angolensis* and unlike *C. machadoi,* in which it is extensive and forked, and *C. namakuiyus*, in which it is extended and unbifurcated). It is distinguished from *C. namakuiyus* by having the intrusion of a scale in broad contact with interparietal and occipitals, thereby separating posterior parietals (*versus* absence of this scale, posterior parietals in full contact, see Fig. 6); a higher number of supralabials (6 in *C. phonolithos* **sp. nov.** *versus* 4–5 in *C. namakuiyus*); a higher number of femoral pores (7 in *C. phonolithos* **sp. nov.** *versus* 4-6 in *C. namakuiyus*); a higher number of generation glands (16–17 in *C. phonolithos* **sp. nov.** *versus* 12 in *C. namakuiyus*); males with fewer caudal scales at the 15th tail whorl (8 in *C. phonolithos* **sp. nov.** *versus* 10 in *C. namakuiyus*); absence of osteoderms on throat and ventral surfaces (*versus* presence), and significantly thicker caudal osteoderms than dorsal osteoderms (resembling *C. machadoi* and *C. angolensis*); temporal scales are weakly keeled (*versus* strongly keeled). In coloration *C. phonolithos* **sp. nov.** is quite similar to *C. namakuiyus*, although the new species has a more vibrant coloration (orange-brown *versus* light brown). It is distinguished from *C. angolensis* by having a large keyhole-shaped interparietal in contact with frontoparietals, thereby separating anterior parietals, with an intrusion of a scale in broad contact with interparietal and occipitals (*versus* small, diamond-shaped interparietal not in contact with frontoparietal, thereby never completely separating anterior parietals, posterior parietals in broad contact, see Fig. 6); fewer ventral transverse scale rows (23 *versus* 27), orange-brown dorsal body coloration (*versus* brown with blackish speckles over paler dorsal ground coloration), and by the absence of a longitudinal series of whitish speckles along dorsal surface (*versus* presence of two longitudinal series of small whitish speckles along dorsum), and presence (*versus* absence) of a loreal.
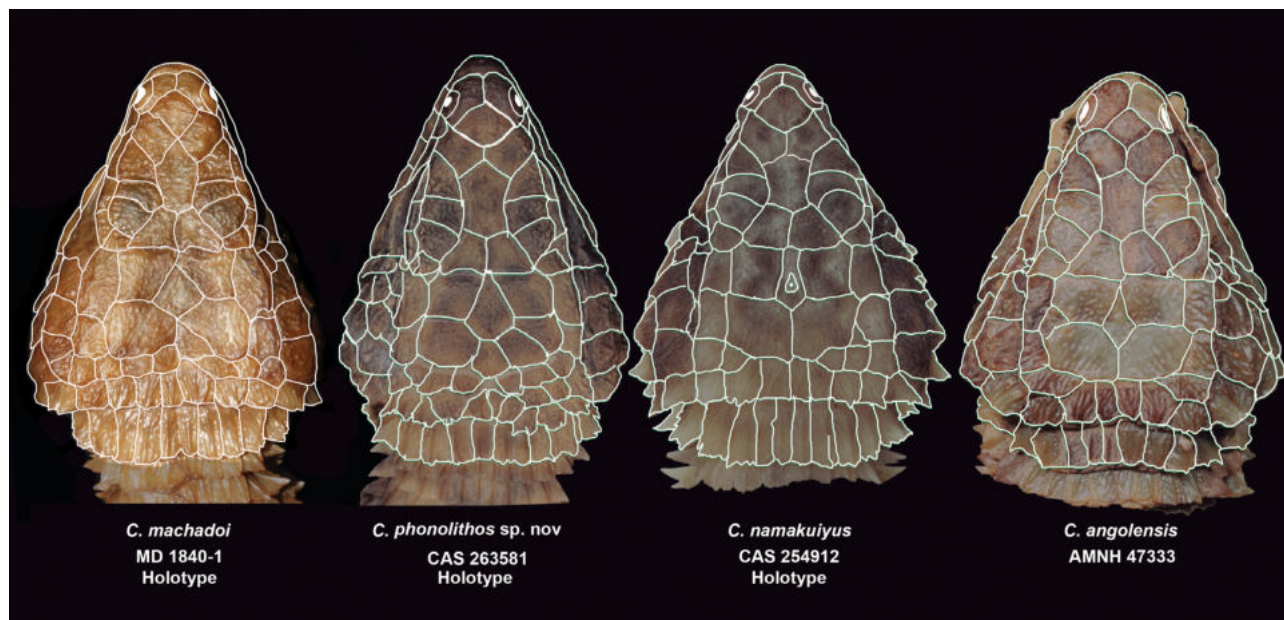

FIGURE 6. Comparison of head scalation between *C. machadoi*, *C. phonolithos* **sp. nov.**, *C. namakuiyus* and C. *angolensis*.

Description of holotype. SVL 71.4 mm. Head and body depressed. Head 1.3 times longer (21.6 mm) than broad (16.5 mm). HH 8.7 mm. SEL 8.2 mm. Nasals in median broad contact; entire frontonasal lozenge-shaped, broader than long, separated from frontal by enlarged prefrontals (in median contact, forming a suture), separated from rostral by nasals, separated from loreal by prefrontals; frontal in contact with first and second supraoculars, followed by a pair of frontoparietals in broad, median contact; a distinctive keyhole-shaped interparietal in broad contact with the frontoparietals, separating anterior parietals; intrusion of a scale in broad contact with interparietal and occipitals, thereby separating posterior parietals; right posterior parietal scale is fragmented; parietal window visible; 10 rugose occipital scales; 10 elongated nuchal scales. Four supraoculars and three supraciliaries. Nasals large, with nostril pierced centrally on upper margin. Loreal in contact with preocular, nasal and first two supralabials; three suboculars, well separated from the lip by the third, fourth and fifth supralabials. Rostral twice as broad as deep; supralabials 6; infralabials 6; chin shields 5. Mental twice as broad as long; gulars smooth, enlarged and forming transverse rows posteriorly, with 17 gulars between the posterior extent of the jaws. Dorsal scales rectangular, rugose, strongly and obtusely keeled; dorsals and laterals in 25 transverse and 23 longitudinal rows; ventrals squarish, smooth, in 23 transverse and 17 longitudinal rows. Scales on dorsum of limbs large, strongly keeled and spinose with thin, non-imbricated osteoderms; subdigital lamellae under fourth toe 15; SAL 28.9 mm. AGD 32.4 mm. HML 9.3 mm, RUL 7.9 mm; FL 12.9 mm; TFL 10.6 mm; LTL 9.8 mm; femoral pores seven; generation glands 16–17. Tail with whorls of large, elongate, strongly keeled, spinose and acuminate scales, spines directed posteriorly; largest spines in dorsolateral position.
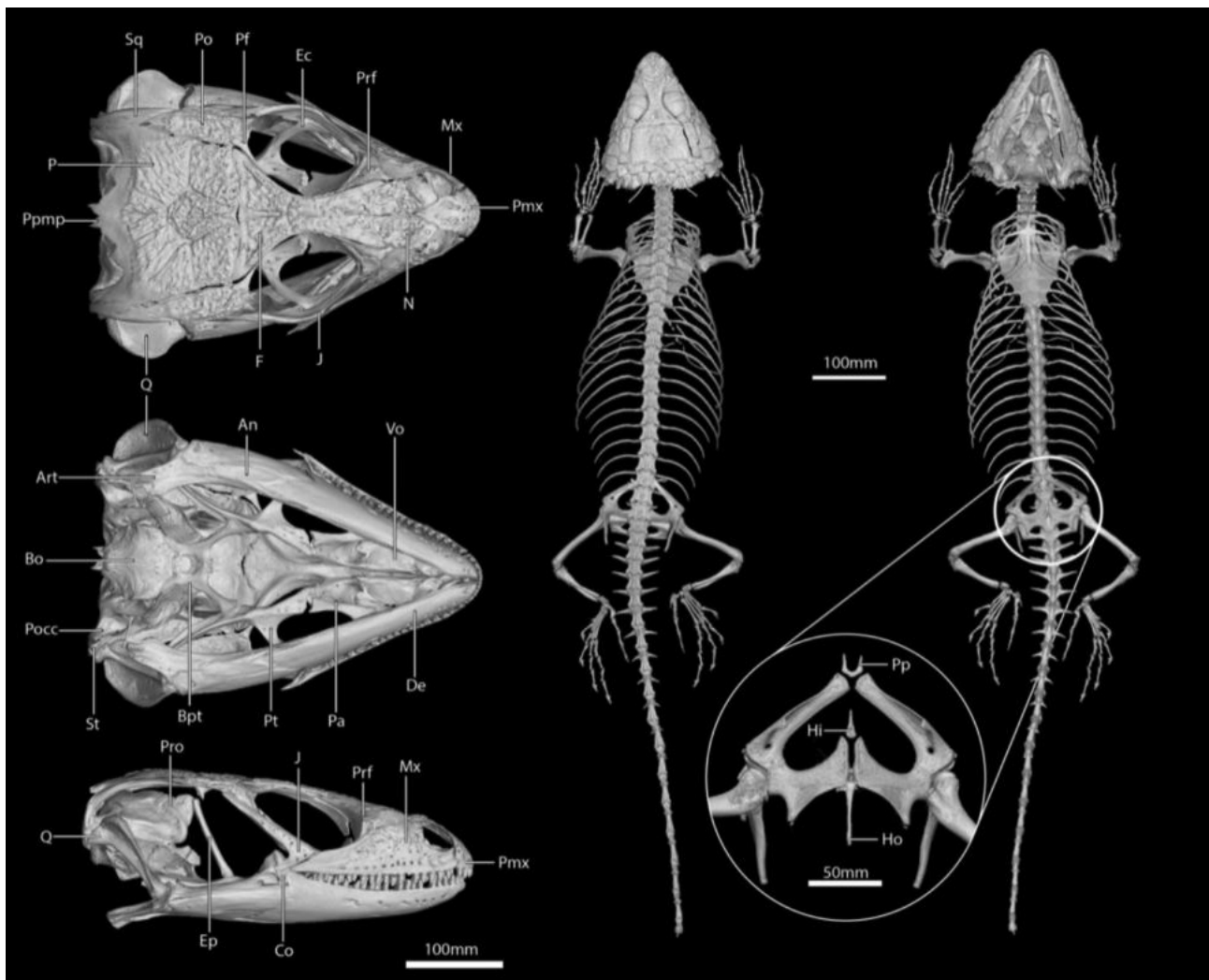
FIGURE 7. Figure showing Cranial and postcranial osteology of CAS 263581 *Cordylus phonolithos* **sp. nov**. holotype. *An*= angular, *Art* = articular, *Bo* = Basioccipital, *Bpt*= Basipterygoid, *Co* = coronoid, *De* = dentary, *Ec* = ectopterygoid, *Ep* = epipterygoid, *F* = frontal, *Hi* = hyperischium, *Ho* = hypoischium, *J* = jugal, *Mx* = maxilla, *N* = nasal, *P* = parietal, *Pa* = Palatine, *Pf* = postfrontal, *Pmx*= premaxilla, *Po* = Postorbital, *Pocc* = paraoccipital, *Pp* = prepubic cartilage, *Ppmp* = posteriomedial process of the parietal, *Prf* = prefrontal, *Pro* = prootic, *Pt* = pterygoid, *Q* = quadrate, *Sq* = squamosal, *St* = supratemporal, *Vo* = vomer.

Cranial osteology. The parietal is pentagonal with two short, well-spaced posteromedial processes bracing a very small, laterally flattened posteriomedial supraoccipital process (Fig. 7). The premaxilla is unpaired and bears seven pleurodont teeth and five foramina, with a dorsal process that extends posteriorly to be clasped by the nasals, which themselves insert into an unpaired frontal posteriorly and prefrontals posterolaterally. The maxilla is typically scinciform, with a deeply grooved crista dentalis and 20 pleurodont teeth. A laminar lacrimal lies medial to the facial process of the maxilla, extending from the posterioventral process of the prefrontal to the anterior process of the jugal. No palpebral is present, though the prefrontal has a small, flattened, laterally projecting tubercle that supports the anteriormost superorbital osteoderm in much the same way. The jugal is triangular in cross-section and asymmetrically T-shaped, with a tapering anterior process and a broad, truncated posterior process that extends along and past the posterior edge of the maxilla. Edentate pterygoids extend back to connect with the quadrates, becoming C-shaped in cross-section posterior to the epipterygoid condyle. The squamosal is curved and blade-like, circular in cross-section anteriorly, becoming flattened posteriorly, where it articulates with the cephalic condyle of the quadrate and the supratemporals. Supratemporals are flattened, sickle-shaped and unfused with the paroccipital processes. The bones of the braincase are unfused, suggesting that this individual may be a subadult. The prootic bears an extended alar process, a well-developed, anteriorly expanded crista prootica, and a very weak supratrigeminal process. Basipterygoid processes are well developed and flattened. The lower jaw has a large adductor fossa, a flattened and medially curved retroarticular process, a medially open Meckelian canal and a dentary with a strong subdental shelf, 22 mandibular teeth, and 11 dentary foramina.
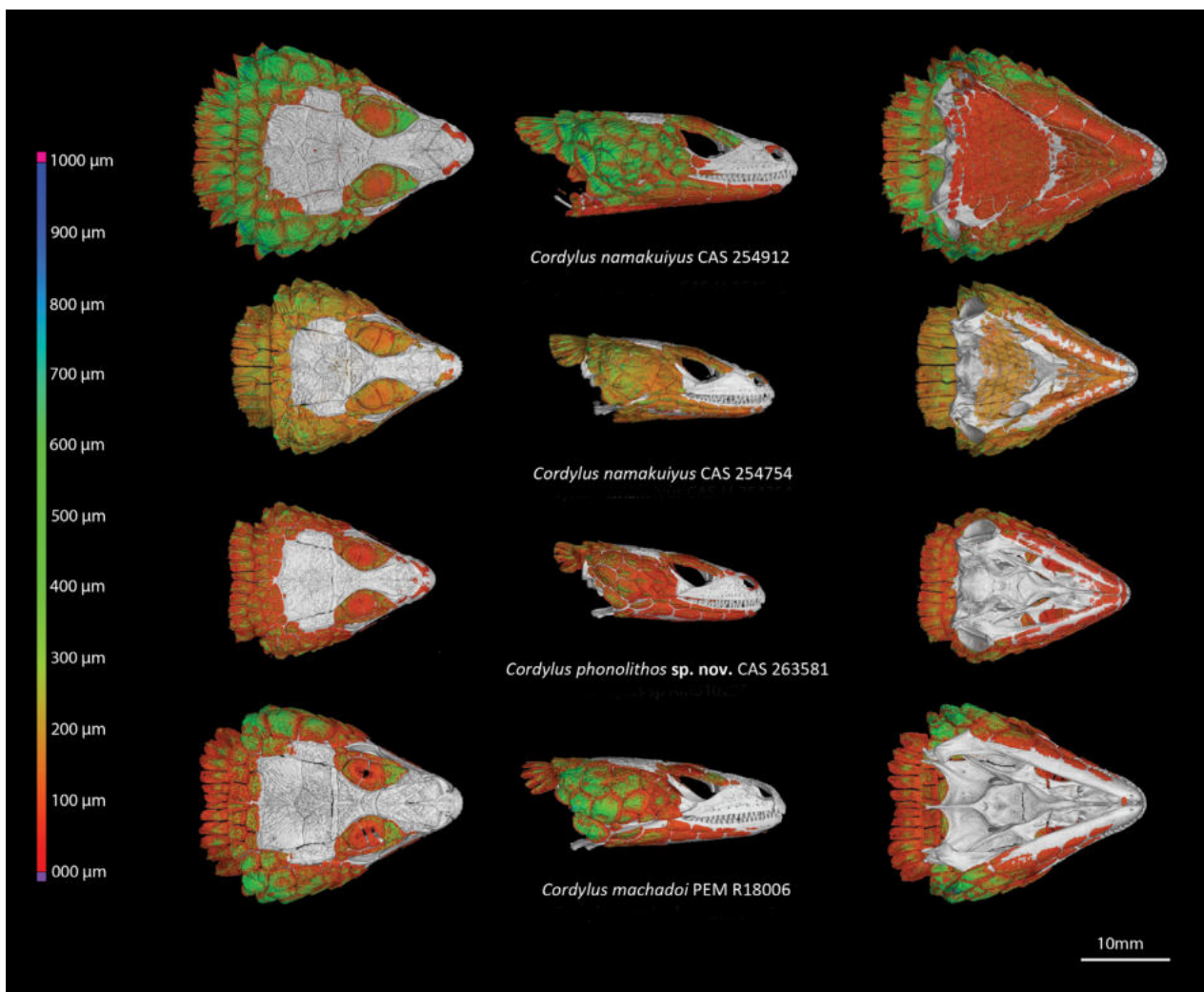
FIGURE 8. Cranial morphology and osteodermal variation on the different Angolan *Cordylus* species, colorized to show cross-sectional thickness.
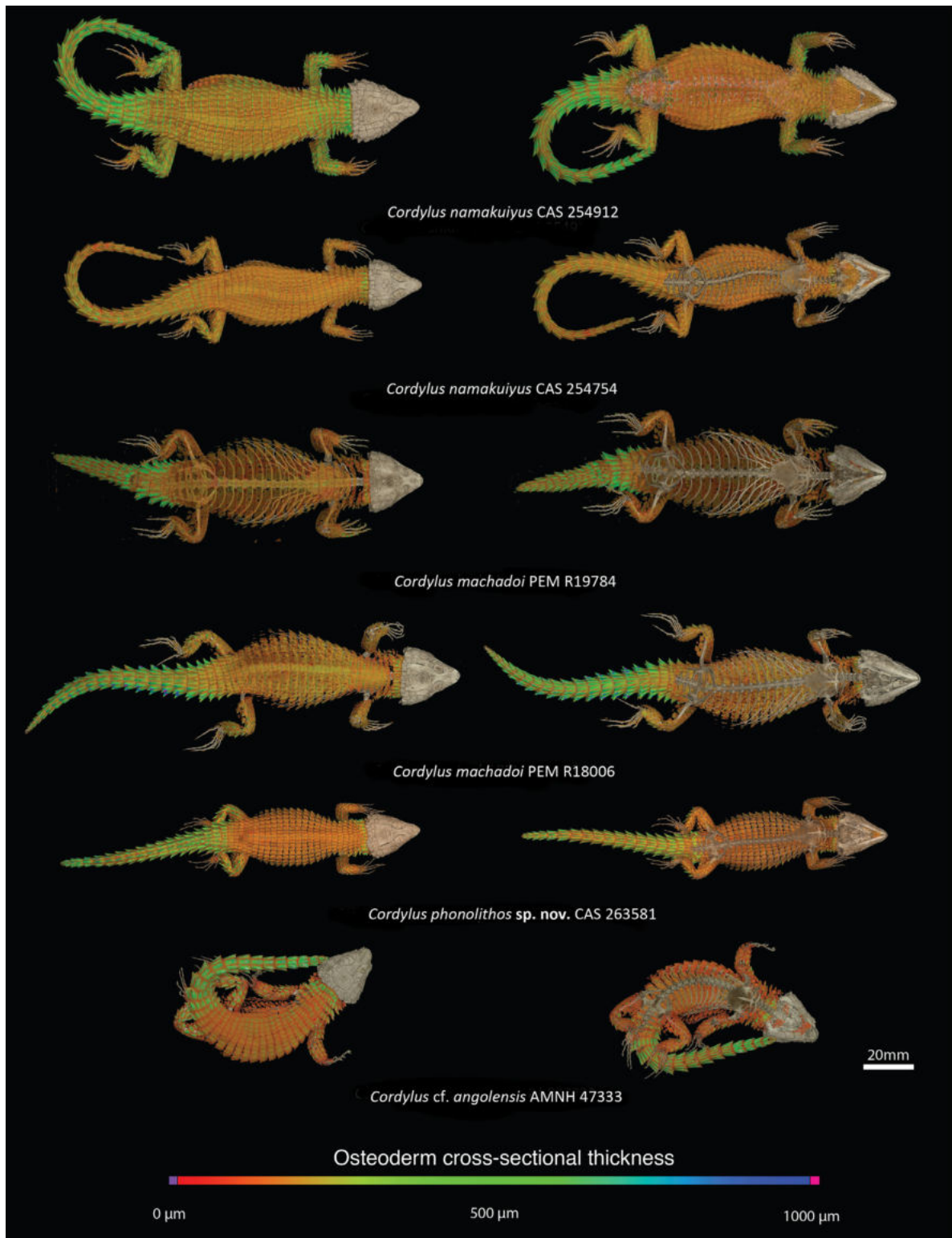
FIGURE 9. Whole body osteodermal variation on the different Angolan *Cordylus* species, colorized to show cross-sectional thickness.

Postcranial osteology. The holotype has 25 presacral, two sacral and 16 postsacral vertebrae (Fig. 7). There are five cervical ribs, three sternal ribs and two xiphisternal ribs. The asternal ribs are asymmetric, with four long ribs with ossified costal cartilage and six short asternal ribs on the left side and five long and seven short ribs on the right. The first three cervical ribs are distally flattened with bifid cartilaginous projections. The pelvic girdle is

MARQUES *ET AL.*

well developed and flattened. No iliac tubercle is present. There is a well-developed, ventrally angled pubic tubercle directly anterior to the obturator foramen. Both hypoischium and hyperischium are well developed. Pubic bones are well separated by a bifurcate prepubic cartilage. The sternal plate is broad and lacks a fontanelle. Interclavicle cruciform, clavicles rod-like and flattened dorsally. The epicoracoid is narrow and curved, connecting the scapular ray to the primary and secondary coracoid rays, but not to the anterior process of the scapular. The condyles of long bones are unfused and the metatarsals and metacarpels are not fully developed, suggesting that this individual is not fully adult. Digits display the typical squamate phalangeal arrangement of 2-3-4-5-3 for the manus and 2-3-4-5-4 for the pes.

Osteoderms. Scales of the dorsal and temporal regions of the skull and the ventrolateral aspects of the jaws are underlain with rugose osteoderms (Fig. 8). These osteoderms are fused to the proximal parietal, frontal and postorbital bones, although the mesokinetic and metakinetic joints appear unobstructed and flexible. The tail, legs and dorsal and lateral aspects of the body are covered in osteoderms (Fig. 9). The dorsal and lateral trunk are protected by noncontiguous, rectangular, 100-200 μm thick osteoderms that become increasingly keeled and mucronate laterally. The caudal osteoderms are significantly thicker (up to 500μm), sharply spined and arranged in imbricate transverse whorls. The whole limbs are covered by imbricate circular/rhomboid osteoderms, keeled and mucronate dorsally, plate-like ventrally. The gular and ventral regions lack osteoderms.

Coloration. Dorsum orange-brown, fading to dirty yellow laterally. Head orange-brown; supralabials and infralabials yellowish; a dark-brown bar extends from the posterior aspect of the eye to the temporals. The base of the tail is brown, with an orange coloration similar to that the laterally that extends towards the tip; dorsum of limbs dark brown. Laterally, a dark-brown line extends from the neck towards the insertion of the forelimbs. The body venter is cream and subcaudal surface is faded orange.

FIGURE 10. Habitat view of the type locality of *Cordylus phonolithos* **sp. nov.** (Photo by Ishan Agarwal).

Table 1. Uncorrected pairwise distances between cordylid taxa for the ND2 mitochondrial gene. All values are presented in percentages (%).

	C. aridus	C. beraduccii	C. cordylus	C. imkeae	C. jonesii	C. machadoi	C. macropholis	C. marunguensis	C. mclachlani	C. minor	C. namakuiyus	C. niger	C. oelofseni	C. phonolithos sp. nov.	C. rhodesianus	C. tropidosternum	C. ukingensis	C. vittifer	O. cataphractus
C. aridus																			
C. beraduccii	20.1																		
C. cordylus	14.3	16																	
C. imkeae	12.2	19.6	11.7																
C. jonesii	19.2	14.7	15.4	18.3															
C. machadoi	18	15.6	16.7	16.9	15.4														
C. macropholis	16.2	18.5	12.4	13.5	16	16.4													
C. marunguensis	18.4	12.1	14.5	17.3	15.5	15	16.4												
C. mclachlani	15.6	18.4	13.4	14.7	18.7	18.3	13	15.4											
C. minor	4.1	17.9	11.6	9.7	17	16.6	13.1	16	12.3										
C. namakuiyus	18	15.4	15.2	15.8	14.3	5.8	16.1	14.7	17.5	15.1									
C. niger	13.3	17.4	10	12.1	15.5	15.6	11.1	15.7	12	10.5	14.1								
C. oelofseni	13.9	15.8	7.1	12.1	15.2	15.1	10.2	14.5	12.3	10.8	14.5	9.1							
C. phonolithos **sp. nov.**	17.9	14.9	16.6	15.2	14.8	7.3	16.8	13.7	18.4	15	6.7	15.2	16.1						
C. rhodesianus	20.3	14.8	15.4	18.5	11.7	14.1	16	13.8	18.2	17.8	13.8	15.3	15	13.8					
C. tropidosternum	18.7	13.1	13.8	16.8	14.6	14.8	16.4	13.6	15.9	15.9	14.2	13.6	14.5	14.9	13.9				
C. ukingensis	19.3	13.6	15	17	15	13.6	14.8	10.4	15.4	15.5	13.7	14.7	14.5	14	15.5	14.4			
C. vittifer	20	14.6	16.5	18.2	15	15.5	18.2	14.8	17.6	17.3	14.7	16.7	16.1	16.8	15.2	15.1	16.1		
O. cataphractus	20.4	17.3	15.8	14.4	17.2	18.1	16	17.6	15.9	13.6	17	15	15	16.1	14.4	16.9	16.1	18.5	

TABLE 2. Variation in meristic counts for specimens of *Cordylus phonolithos* **sp. nov.**, *C. namakuiyus*, *C. machadoi* and *C. angolensis*. All measurements are presented in millimeters (mm). Data of *C. namakuiyus* retrieved from Stanley *et al.* (2016); data for *C. machadoi* retrieved from Stanley *et al.* (2016) and two additional specimens from this study; data for *C. phonolithos* **sp. nov.** and *C. angolensis* collected in this study.

	Cordylus phonolithos sp. nov.		*Cordylus namakuiyus*			*Cordylus machadoi*			*Cordylus angolensis*		
	Male n=1 (Holotype)	Juvenile n=1 (Paratype)	Female n=5	Male n=1	Juvenile n=4	Female n=6	Male n=5	Juvenile n=5	Female n=1	Male n=1	Juvenile n=1
Maximum SVL	71.4	49.9	101.9	89.7	57.1	97.8	94.2	66.7	79.5	78.2	61.9
Chin Shields	5	5	5–6	5	5	5	5	5	5	5	5
Femoral Pores	7	0	5	5	0–6	6–7	5–7	5–6	5	5	5
Generation Glands	17–13	0	0	12	0	0	12–22	0–16	0	36	0
Supralabials	6	6	4–5	5	5	5	5	5	4–5	4–5	4
Infralabials	6	6	5–6	5	5	6	6	5	5	5	5
Supraoculars	4	4	4	4	4	4	4	4	4	4	4
Supraciliars	3	3	3	3	3	3	3	3–4	3	3	3
Loreal	1	FUSED	0–1	1	1	1	1	1	1	1	1
Suboculars	3	3	2–3	3	3	3–4	3	3	2–3	3	2–3
Preoculars	1	FUSED	1	1	1	1	1	1	1	1	1
Transverse Gular Scales	17	17	14–17	15	15–16	17–21	18–20	18–24	18	18	18
Dorsal Transverse Rows	25	25	24–26	24	23–25	24–28	23–26	25–28	22	21	21
Dosolateral Longitudinal Rows	23	23	24	23	23–24	22–27	23	23–24	18–19	18–19	18–19
Ventral Transverse Rows	23	23	21–24	22	21–22	21–25	21–26	20–22	25–26	25	24
Ventral Longitudinal Rows	17	17	15–16	17	14–16	14–18	13–16	13–14	12	12	11
Caudal Scales 11th Whorl	10	10	10–12	10	10	10–11	10	10	10	11	11
Caudal Scales 15th Whorl	8	8	10	10	10	8–10	10–11	9	8	0	0
Subdigital Lamellae F1: F2: F3:	4: 8: 10:	–	5–6: 7–9:	6: 8:	5–6:	5: 8–9:	4–6:	5–6: 8–9:	4: 8: 11: 12: 5	4: 9:	4: 8: 11:
F4: F5	12: 8		10–12: 11–13: 7–9	11: 12: 8	9–10: 11–12: 12–13: 8–9	11–12: 11–13: 8–9	7–9: 9–11: 9–11: 7.9	11: 11: 8		11: 12: 4	12: 0
Subdigital Lamellae T1: T2:	6: 9: 11: 14:	–	5–7: 8–10:	6: 9:	5–7: 8–10:	6: 8–10:	5: 8–9:	6: 9–10:	19: 10: 12:13:	9: 11:	–
T3: T4: T5	10		11–12: 13–14: 10–11	11: 13: 11	11–14: 14– 17: 10–12	12–13: 12–15: 10–12	10–12: 11–14: 9–11	11–12: 14: 10–11	10	11: 12: 9	

Variation. Variation in meristic counts of the type series is reported in Table 2. The single juvenile paratype agrees almost entirely with the holotype, although, the loreal and the preocular scales are fused and the right posterior parietal is entire. Measurements of the paratype are the following: SVL 49.9 mm; HL 15.2 mm; HW 10.7 mm; HH 6.4 mm; SEL 5.8 mm; SAL 20.2 mm; AGD 23.1 mm; HML 6 mm; RUL 5.4 mm; FL 7.9 mm; TFL 7.8 mm; LTL 8 mm.

Distribution. The new species is known only from N'Dolondolo, at the base of the Serra de Neve Inselberg in Namibe Province, Angola. The observational record cited by Stanley *et al.* (2016), originally identified as *C. namakuyius* from "Sera [sic] de Neve" (= Serra da Neve) is likely to correspond to *C. phonolithos* **sp. nov**.

Habitat and Natural history notes. This species was found in granite outcrops in "sparse Miombo" forest (Fig. 10), dominated by trees of the genera *Brachystegia* and *Jubernardia* (Grandvaux-Barbosa 1970). The juvenile paratype was found under a small granite rock on a larger rock, while the holotype was collected from within a crevice in a granite boulder. The latter was exposed outside of the crevice, quickly sheltering in response to our presence. CT scanning of the holotype revealed a myriapod carapace in its digestive tract.

Etymology. The specific epithet "*phonolithos*" is a noun in apposition from the Greek "*phono*" = sound + "*lithos*" = rock, which means "sound stone". In the local Mucobal language the type locality name, "N'Dolondolo" means literally "rock that sounds like a bell" or "bell" and stems from the presence of a large and famous phonolite stone at the locality. Phonolites are rare igneous volcanic stones of intermediate composition between felsic and maphic, with aphanitic to porphyritic texture that produce a very distinctive metallic sound when hit, similar to the ringing of a metallic bell. We suggest "N'Dolondolo Girdled Lizard" and "Lagarto Espinhoso de N'Dolondolo" as the English and Portuguese common names, respectively, for this species.

Discussion

The morphological and phylogenetic data presented in this study provide evidence that, although well nested within the Angolan *Cordylus* lineage, the species from Serra da Neve represents a distinct species from the escarpment-dwelling *C. machadoi* and from the low-elevation species *C. namakuiyus*. The newly described species is sister to the lineage containing *C. machadoi* and *C. namakuiyus*. This relationship is not surprising. Although Serra da Neve represents an isolated inselberg, separated from the escarpment by about 100 km of lowlands, the type of habitat on the inselberg is much more similar to that of the escarpment. Both are dominated by Miombo forest, contrasting with the Mopane savanna of the surrounding lowlands. A few other escarpment taxa, e.g. *Agama schacki* Mertens, 1938 and *Trachylepis ansorgii* Boulenger, 1907 also occur there. Other taxa more typical of the northern regions of the country, such as *Panaspis cabindae* (Bocage, 1866), also find suitable habitat in the inselberg. However, the inselberg is also home to typically low-elevation taxa like *Trachylepis laevis* (Boulenger, 1907) or *Poyntonophrynus grandisonae* (Poynton & Haacke, 1993). Although our knowledge of the biogeographic affinities of Serra da Neve is still incomplete, it may be hypothesized that a combination of a steep elevation gradient and geographic position allow this inselberg to support both lowland and escarpment adapted animals.

The discovery of *C. phonolithos* **sp. nov.** combined with the recent description of *Poyntonophrynus pachnodes* from Serra da Neve, flags the importance of this particular inselberg in terms of biodiversity and endemicity. Documented richness and endemicity are likely to increase in the next few years, as a few other species of lizards, currently only known from Serra da Neve, are being described (Marques *et al.* in prep.), and further expeditions are likely to increase the numbers of known taxa for the region. Despite being situated in Namibe Province and in close proximity to Benguela Province, two of the most well-known and herpetologically diverse areas of the country (Marques *et al.* 2018), the biodiversity of Serra da Neve remains largely undocumented. Isolated inselbergs across Africa display a remarkable degree of endemism, a pattern exemplified by the species of reptiles that have been recently described from northern Mozambique (Branch *et al.* 2005; Branch & Bayliss 2009; Branch & Tolley 2010; Portik *et al.* 2013; Branch *et al.* 2014).

Being heterogeneously distributed in the landscape and rising abruptly from the surrounding ecological matrix, inselbergs represent independent ecosystems, which have an important role as refugia and in population diversification and structuring, supporting a variety of microhabitats and different faunal and floral communities (Porembski & Barthlott 2000; Porembski *et al.* 2000; Porembski 2007; Bruke 2003, 2005; Brand 2011; Bayliss *et al.* 2014). These "terrestrial islands" are known to support an exceptional diversity of both animals and plants (Simons *et al.* 1998; Porembski & Barthlott 2000; Bruke 2001; Michael *et al.* 2008; Bayliss *et al.* 2014).

MARQUES *ET AL.*

The rich and unique biodiversity of inselbergs are often of elevated conservation interest. This is partly due to their limited area and isolation which makes them particularly vulnerable to external pressures, such as landscape changes and degradation, invasive species, pollution and especially climate change (Porembski & Barthlott 2000). Other similar inselbergs in Angola —Mount Moco in Huambo Province for example— have suffered considerable impacts, namely due to habitat destruction resulting from deforestation for charcoal production and agricultural practices (Mills *et al.* 2011; Gonçalves *et al.* 2019). The anthropogenic impact we observed at Serra da Neve is still minimal. The local human population uses old volcanic craters at higher elevations for small-scale agriculture. No extensive charcoal production was observed, although hunting and honey production appear to be common practices. Cattle are still confined to the areas at the base of Serra da Neve, mostly related to the traditional nomadic pastoralism of the Mucobal people. Habitat preservation at Serra da Neve, when compared to other parts of the country, can certainly be attributed to the lack of easy access either to the base of the mountain, or especially the plateau. Indeed, some isolated cliffs have no access at all. However, given the rapid growth of human population in the region and constant demands for charcoal in other parts of the country, this situation could rapidly be altered, emphasizing the need to consider conservation plans for the area. Serra da Neve has been highlighted by Huntley & Matos (1994) as an area of particular conservation interest, and the establishment of a conservation area is currently being considered by the Ministry of Environment. The very limited available biological data regarding *Cordylus phonolithos* **sp. nov.** require a Data Deficient listing, following the IUCN Red List guidelines. Taxa listed as Data Deficient should be treated with special concern and given priority in terms of studies and conservation efforts (IUCN 2001). However, due to its limited geographic distribution and apparent endemicity to the Serra da Neve Inselberg, it is likely that in the future a threatened or endangered classification may have to be adopted.

References

Baptista, N., António, T. & Branch, W.R. (2018) Amphibians and reptiles of the Tundavala region of the Angolan Escarpment. *Biodiversity & Ecology*, 6, 397–403.
https://doi.org/10.7809/b-e.00351

Barker, N., Clark, R., Neef, G., Maiato, F., Francisco, D. & Goyder, D. (2015) Learning the ABC's: Angolan botanical collecting—part 2: bush pilots and old volcanoes. *Veld & Flora*, 101 (3), 116–119.

Bayliss, J., Timberlake, J.R., Branch, W.R., Bruessow, C., Collins, S., Congdon, C., Curran, M., de Sousa, C., Dowsett, R.J., Dowsett-Lemaire, F., Fishpool, L.D.C., Harris, T., Georgiardis, S., Kopp, K., Liggitt, B., Monadjem, A., Patel, H., Ribeiro, D., Spottiswoode, C., Taylor, P., Willcock, S. & Smith, P. (2014) The discovery, biodiversity and conservation of Mabu forest—the largest mid-altitude rainforest in southern Africa. *Oryx*, 48, 177–185.
https://doi.org/10.1017/S0030605313000720

Biton, D.T. (2014) Two new water beetles from the Hantamsberg, an inselberg in the Northern Cape of South Africa (Coleoptera, Hydraenidae). *Zootaxa*, 3887 (4), 471–480.
https://doi.org/10.11646/zootaxa.3887.4.5

Bocage, J.V.B. (1895) *Herpétologie d'Angola et du Congo*. Ministério da Marinha e das Colónias, Lisbonne, 203 pp., 20 pls.

Branch, W.R. (1998) *Field Guide to Snakes and Other Reptiles of Southern Africa*, 3rd edition. Ralph Curtis Books, Sanibel Island, Florida, 399 pp.

Branch, W.R. & Bayliss, J. (2009) A new species of *Atheris* (Serpentes: Viperidae) from northern Mozambique. *Zootaxa*, 2113 (1), 41–54.
https://doi.org/10.11646/zootaxa.2113.1.2

Branch, W.R. & Tolley, K.A. (2010) A new species of chameleon (Sauria: Chamaeleonidae: *Nadzikambia*) from Mount Mabu, central Mozambique. *African Journal of Herpetology*, 59, 157–172.
https://doi.org/10.1080/21564574.2010.516275

Branch, W.R., Rödel, M.-O. & Marais, J. (2005) A new species of rupicolous *Cordylus* Laurenti 1768 (Sauria: Cordylidae) from Northern Mozambique. *African Journal of Herpetology*, 54, 131–138.
https://doi.org/10.1080/21564574.2005.9635526

Branch, W.R., Bayliss, J. & Tolley, K.A. (2014) Pygmy chameleons of the *Rhampholeon platyceps* complex (Squamata: Chamaeleonidae): Description of four new species from isolated 'sky islands' of northern Mozambique. *Zootaxa*, 3814 (1), 1–36.
https://doi.org/10.11646/zootaxa.3814.1.1

Branch, W.R., Vaz Pinto, P., Conradie, W. & Haacke, W.D. (2014) Reptile diversity in southwest Angola. *Abstracts and Program of the 12th Herpetological Association of Africa*, 2014, 4.

Brand, R.F., Brown, L.R. & Du Preez, P.J. (2011) Biogeography of Platberg, Eastern Free State, South Africa: links with Afromontane regions and South African biomes. *In*: Grillo, O. & Venora, G. (Eds.), *Biodiversity Loss in a Changing Planet*. InTech Publisher International, Rijeka, pp. 113–136.

Broadley, D.G. & Mouton, P. le F.N. (2000) A new species of rupicolous *Cordylus* Laurenti from Malawi (Sauria: Cordylidae). *African Journal of Herpetology*, 49, 169–172.
https://doi.org/10.1080/21564574.2000.9635443

Broadley, D.G. & Branch, W.R. (2002) A review of the small east African *Cordylus* (Sauria: Cordylidae), with the description of a new species. *African Journal of Herpetology*, 51, 9–34.
https://doi.org/10.1080/21564574.2002.9635459

Bruke, A. (2001) Determinants of inselberg floras in arid Nama Karoo landscapes. *Journal of Biogeography*, 28, 1211–1220.
https://doi.org/10.1046/j.1365-2699.2001.00623.x

Bruke, A. (2003) The role of Namibian inselbergs in contributing to local and regional plant species richness. *Biodiversity and Conservation*, 12, 469–486.
https://doi.org/10.1023/A:1022491723262

Bruke, A. (2005) Biodiversity patterns in arid, variable environments, a case study of Namibian Inselberg and Mountain Flora. *Mountain Research and Development*, 25, 228–234.
https://doi.org/10.1659/0276-4741(2005)025[0228:BPIAVE]2.0.CO;2

Butler, B.O., Ceríaco, L.M.P., Marques, M.P., Bandeira, S., Júlio, T., Heinicke, M. & Bauer, A.M. (2019) Herpetological survey of Huíla Province, Southwest Angola, including first records from Bicuar National Park. *Herpetological Review*, 50 (2), 225–240.

Ceríaco, L.M.P., de Sá, S.A.C., Bandeira, S., Valério, H., Stanley, E.L., Khun, A.L., Marques, M.P., Vindum, J.V., Blackburn, D.C. & Bauer, A.M. (2016) Herpetological survey of Iona National Park and Namibe Regional Natural Park, with a synoptic list of the amphibians and reptiles of Namibe Province, southwestern Angola. *Proceedings of the California Academy of Sciences*, Series 4, 63, 15–61.

Ceríaco, L.M.P, Marques, M.P., Bandeira, S., Agarwal, I., Stanley, E.L., Bauer, A.M., Heinicke, M.P. & Blackburn, D.C. (2018) A new earless species of *Poyntonophrynus* (Anura, Bufonidae) from the Serra da Neve Inselberg, Namibe Province, Angola. *ZooKeys*, 780, 109–136.
https://doi.org/10.3897/zookeys.780.25859

Congdon, T.C.E., Collins, S. & Bayliss, J. (2010) Butterflies of south-east Africa's mountains (Mozambique and Malawi). *Metamorphosis*, 21 (2), 45–107.

Conradie, W., Measey, G.J., Branch, W.R. & Tolley, K.A. (2012) Revised phylogeny of African sand lizards (*Pedioplanis*), with the description of two new species from south-western Angola. *African Journal of Herpetology*, 61, 91–112.
https://doi.org/10.1080/21564574.2012.676079

Conradie, W., Bittencourt-Silva, G.B., Farooq, H.M., Loader, S.P., Menegon, M. & Tolley, K.A. (2018) New species of mongrel frogs (Pyxicephalidae: *Nothophryne*) for northern Mozambique inselbergs. *African Journal of Herpetology*, 67, 61–85.
https://doi.org/10.1080/21564574.2017.1376714

Daniels S.R. & Bayliss, J. (2012) Neglected refugia of biodiversity: mountainous regions in Mozambique and Malawi yield two novel freshwater crab species (Potamonautidae: *Potamonautes*). *Zoological Journal of the Linnaean Society*, 164, 498–509.
https://doi.org/10.1111/j.1096-3642.2011.00773.x

Daniels, S., Phiri, E. & Bayliss, J. (2014) Renewed sampling of inland aquatic habitats in southern Africa yields two novel freshwater crab species (Decapoda: Potamonautidae: *Potamonautes*). *Zoological Journal of the Linnaean Society*, 171, 356–369.
https://doi.org/10.1111/zoj.12139

Edgar, R.C. (2004) MUSCLE: Multiple sequence alignment with high accuracy and high throughput. *Nucleic Acids Research*, 32, 1792–1797.
https://doi.org/10.1093/nar/gkh340

Felsenstein, J. (1895) Confidence limits on phylogenies: an approach using the bootstrap. *Evolution*, 39, 783–791.
https://doi.org/10.2307/2408678

Grandvaux-Barbosa L.A. (1970) *Carta fitogeoráfica de Angola*. Instituto de Investigação Científica de Angola, Luanda, 323 pp.

Greenbaum, E., Stanley, E.L., Kusamba, C., Moninga, W.M., Goldberg, S.R. & Bursey, C.R. (2012) A new species of *Cordylus* (Squamata: Cordylidae) from the Marungu Plateau of south-eastern Democratic Republic of the Congo. *African Journal of Herpetology*, 61, 14–39.
https://doi.org/10.1080/21564574.2012.666505

Gonçalves, F.M.P., Braine, D., Bauer, A.M., Valério, H., Marques, M.P. & Ceríaco, L.M.P. (2019) Rediscovery of the poorly known Angolan Adder, *Bitis heraldica* (Bocage, 1889) (Serpentes: Viperidae): New records, live photographs and first case history of envenomation. *Herpetological Review*, 50 (2), 241–246.

Huelsenbeck, J.P. & Hillis, D.M. (1993) Success of phylogenetic methods in the four-taxon case. *Systematic Biology*, 42, 247–264.
https://doi.org/10.2307/2992463

Huntley, B. & Matos, E.M. (1994) Botanical diversity and its conservation in Angola. *Strelitzia*, 1, 53–74.

IUCN (2001) *IUCN Red List Categories and Criteria. Version 3.1. 2ⁿᵈ Edition*. IUCN, Gland and Cambridge, iv + 32 pp.

Kumar, S., Stecher, G., Li, M., Knyaz, C. & Tamura, K. (2018) MEGA X: Molecular Evolutionary Genetics Analysis across computing platforms. *Molecular Biology and Evolution*, 35, 1547–1549.
https://doi.org/10.1093/molbev/msy096

Linder, H.P., de Klerk, H.M., Born, J., Burgess, N.D., Fjeldsta, J. & Rahbek, C. (2012) The partitioning of Africa: Statistically defined biogeographical regions in sub-Saharan Africa. *Journal of Biogeography*, 39, 1189–1205.
https://doi.org/10.1111/j.1365-2699.2012.02728.x

Loveridge, A. (1944) Revision of the African lizards of the family Cordylidae. *Bulletin of the Museum of Comparative Zoölogy*, 95, 1–118, pls. 1–12.

Marques, M.P., Ceríaco, L.M.P., Blackburn, D.C. & Bauer, A.M. (2018) Diversity and distribution of the amphibians and terrestrial reptiles of Angola—Atlas of historical and bibliographic records (1840–2017). *Proceedings of the California Academy of Sciences*, Series 4, 65 (supplement 2), 1–501.

Michael, D.R., Cunningham, R.B. & Lindenmayer, D.B. (2008) A forgotten habitat? Granite inselbergs conserve reptile diversity in fragmented agricultural landscapes. *Journal of Applied Ecology*, 45, 1742–1752.
https://doi.org/10.1111/j.1365-2664.2008.01567.x

Miller, M.A., Pfeiffer, W. & Schwartz, T. (2010) Creating the CIPRES Science Gateway for inference of large phylogenetic trees. *Proceedings of the Gateway Computing Environments Workshop (GCE)*, *New Orleans, Louisiana*, 14 November 2010, 1–8.
https://doi.org/10.1109/GCE.2010.5676129

Mills, M.S.L., Olmos, F., Melo, M., Richard, W. & Dean, J. (2011) Mount Moco: its importance to the conservation of Swierstra's Francolin *Pternistis swierstrai* and the Afromontane avifauna of Angola. *Bird Conservation International*, 21 (2), 119–133.
https://doi.org/10.1017/S0959270910000493

Monadjem A., Schoeman, M.C., Reside, A., Pio, D.V., Stoffberg, S., Bayliss, J., Cotterill, F.P.D., Curran, M., Kopp, M. & Taylor, P.J. (2010) A recent inventory of the bats of Mozambique with documentation of seven new species for the country. *Acta Chiropterologica*, 12, 371–391.
https://doi.org/10.3161/150811010X537963

Nielsen, S.V. & Colston, T.J. (2014) The phylogenetic position of Ethiopia's sole endemic and biogeographically enigmatic cordylid lizard, *Cordylus rivae* (Squamata: Cordylidae), and a discussion of its conservation status. *African Journal of Herpetology,* 63, 166–176.
https://doi.org/10.1080/21564574.2014.953606

Nylander, J.A.A. (2008) *MrModeltestv2.3*. Program distributed by the author. Evolutionary Biology Center, Uppsala University, Uppsala.[Program]

Pereira, E. (1977) Serra da Neve (Angola)—Nota sobre a geomorfologia da região e idade das aplanações. *Boletim da Sociedade Geológica de Portugal*, 20, 277–282.

Pereira, E. & Moreira, A. (1977) Sobre o complexo de estruturas anelares da Serra da Neve (Angola). *In*: II Centenário da Academia das Ciências de Lisboa. *Reconhecimento Científico de Angola: Estudos de Geologia e Paleontologia e de Micologia*. Academia das Ciências de Lisboa, Lisboa, pp. 97–120.

Porembski, S. (2007) Tropical inselbergs: habitat types, adaptive strategies and diversity patterns. *Brazilian Journal of Botany*, 30, 579–586.
https://doi.org/10.1590/S0100-84042007000400004

Porembski, S. & Barthlott, W. (2000) Granitic and gneissic outcrops (inselbergs) as centers of diversity desiccation-tolerant vascular plants. *Plant Ecology*, 151, 19–28.
https://doi.org/10.1023/A:1026565817218

Porembski, S., Becker, U. & Seine, R. (2000) Islands on islands: habitats on inselbergs. *In*: Porembski, S. & Barthlott, W. (Eds.), *Inselbergs—Biotic Diversity of Isolated Rock Outcrops in Tropical and Temperate Regions*. Springer-Verlag, Berlin, pp. 49–67.
https://doi.org/10.1007/978-3-642-59773-2_4

Portik, D.M., Travers, S.L., Bauer, A.M. & Branch, W.R. (2013) A new species of *Lygodactylus* (Squamata: Gekkonidae) endemic to Mount Namuli, an isolated 'sky island' of northern Mozambique. *Zootaxa*, 3710 (5), 415–435. https://doi.org/10.11646/zootaxa.3710.5.2

Poynton, J.C. & Broadley, D.G. (1978) The herpetofauna. *In:* Werger, M.J.A & van Bruggen, A.C. *Biogeography and Ecology of Southern Africa*. Dr. W. Junk Publishers, The Hague, pp. 927–948. https://doi.org/10.1007/978-94-009-9951-0.

Ronquist, F., Teslenko, M., van der Mark, P., Ayres, D.L., Darling, A., Höhna, S., Larget, B., Liu, L., Suchard, M.A. & Huelsenbeck, J.P. (2012) MrBayes 3.2: Efficient Bayesian Phylogenetic Inference and Model Choice Across a Large Model Space. *Systematic Biology*, 61 (3), 539–542. https://doi.org/10.1093/sysbio/sys029

Stamatakis, A. (2006) RAxML-VI-HPC: maximum likelihood-based phylogenetic analyses with thousands of taxa and mixed models. *Bioinformatics*, 22, 2688–2690. https://doi.org/10.1093/bioinformatics/btl446

Stanley, E.L., Bauer, A.M., Jackman, T.R., Branch, W.R. & Mouton, P. le F.N. (2011) Between a rock and a hard polytomy: Rapid radiation in the rupicolous girdled lizards (Squamata: Cordylidae). *Molecular Phylogenetics and Evolution*, 58, 53–70. https://doi.org/10.1016/j.ympev.2010.08.024

Stanley, E.L., Ceríaco, L.M.P., Bandeira, S., Valerio, H., Bates, M.F. & Branch, W.R. (2016) A review of *Cordylus machadoi* (Squamata: Cordylidae) in southwestern Angola with the description of a new species from the Pro-Namib desert. *Zootaxa*, 4061 (3), 201–226. https://doi.org/10.11646/zootaxa.4061.3.1

Simmons, R.E., Griffin, M., Griffin, R.E., Marais, E. & Kolberg, E. (1998) Endemism in Namibia: patterns, processes and predictions. *Biodiversity and Conservation*, 7, 513–530. https://doi.org/10.1023/A:1008879712736

Taylor, P.J., Stoffberg, S., Monadjem, A., Schoeman, M.C., Bayliss, J. & Cotterill, F.P.D. (2012) Four new bat species (*Rhinolophus hildebrandtii* complex) reflect Plio-Pleistocene divergence of dwarfs and giants across an afromontane archipelago. *PLoS ONE*, 7, e41744. https://doi.org/10.1371/journal.pone.0041744

Uetz, P., Freed, P. & Hošek, J. (2019) The Reptile Database. Available from: http://www.reptile-database.org (accessed 6 April 2019)

APPENDIX 1. Material used for the description of *Cordylus phonolithos* **sp. nov.** including specimens used in both morphological and molecular analyses (genotyped specimens are indicated with an asterisk). All coordinates are presented in WGS-84 datum.

Institutional Abbreviations: American Museum of Natural History (AMNH); California Academy of Sciences (CAS); Ditsong National Museum of Natural History (TM); Instituto Nacional da Biodiversidade e Áreas de Conservação (INBAC/AMB); Museu Regional do Dundo (MD); Museum of Comparative Zoology (MCZ); National Museum of Namibia (NMN); Port Elizabeth Museum (PEM).

ANGOLA

Cordylus phonolithos **sp. nov.:** CAS 263581* (holotype), INBAC/AMB 10272* (paratype) "rock in vicinity of Ndolondolo, Namibe Prov." [-13.8067º, 13.13507º].

Cordylus namakuyius: CAS 254912* (holotype), CAS 254913 (paratype), CAS 254914 (paratype), CAS 256529* (paratype) "Namibe-Lubango Rd, rd marker 59, 1.8 km W (by rd) of Caraculo, N side of rd, Namibe Prov." [-15.47589º, 12.46269º]; CAS 254754* (paratype), CAS 254755* (paratype), CAS 256530* (paratype), CAS 256531* (paratype) "7.35 km NW (by rd) of Pico Azevedo, Namibe Prov." [-15.47589º, 12.46269º]; PEM R18005* (paratype) "Road from Namibe to Omahua lodge, Namibe Prov." [-15.99681º, 12.40683º]; AMNH 47301 "Angola"; TM 40430 "49 km ESE of Tombua, Namibe Prov." [-15.88333º, 12.26667º].

Cordylus machadoi: CAS 263578, 263579 "Tundavala, Huíla Prov." [-14.823859º, 13.381138º]; MCZ R74120 (paratype) "Leba, Boca da Humpata, Huíla Prov." [-15.083º, 13.267º]; MD 1840-1 (holotype) "Leba, Humpata, environs de Sá da Bandeira" [-15.083 N, 13.267 E, WGS-84]; TM 40095, TM 40096 "5 km S of Chibemba" [-15.75000º, 14.08333º]; TM 40131, TM 40132, TM 40133 "12 km E of Humbia" [-16.674635º, 15.033388º] (= 12 km E of Humbe); PEM R18006, PEM R18007, PEM R18008*, PEM R19782, PEM R19784* "Humpata environs, Huíla Prov." [-14.96186º, 13.33497º], PEM R18009*, NMN 7002 "Nasecute do Tchiviuguira, Huíla Prov." (= Nascente do Tchivinguiro) [-15.01747º, 13.32089º].

Cordylus angolensis: AMNH 47333, AMNH 47334, AMNH 47335 "Mombolo, Kwanza Sul Prov." [-11.9166º, 14.85000º].

Supplementary Material 1. CT-Scan settings.

Taxa	Accession #	Element	Voxel resolution	X-ray kV	X-ray mA	X-ray Watts	Detector time	Filter	Number of rotations	averaging	DOI
Cordylus phonolithos **sp. nov.**	CAS 263581	Skeleton	0.04911535	100	200	20	0.200098	none	1800	3	doi:10.17602/M2/M75155
Cordylus phonolithos **sp. nov.**	CAS 263581	Skull	0.01019516	75	150	11.25	0.200098	none	1100	3	doi:10.17602/M2/M75156
Cordylus namakuiyus	CAS 254754	Skull	0.0135124	90	160	14.4	0.200098	0.1 mm Cu	1400	3	
Cordylus namakuiyus	CAS 254754	Skeleton	0.05308188	100	200	20	0.200098	0.1 mm Cu	1200	3	
Cordylus namakuiyus	CAS 254755	Skull	0.0135708	90	160	14.4	0.200098	0.1 mm Cu	2200	3	
Cordylus namakuiyus	CAS 254755	Skeleton	0.06209304	120	200	24	0.200098	none	2000	3	
Cordylus namakuiyus	CAS 254912	Skull	0.0124149	140	140	19.6	1	0.1 mm Cu	1200	3	doi:10.17602/M2/M75178
Cordylus namakuiyus	CAS254912	Skeleton	0.07953507	100	200	20	0.200098	none	1800	3	doi:10.17602/M2/M75176
Cordylus namakuiyus	CAS 254913	Skull	0.01936437	70	290	20.3	0.200103	0.5 mm Cu	1000	3	
Cordylus namakuiyus	CAS 254913	Skeleton	0.13735179	120	150	18	0.333096	none	1000	3	
Cordylus namakuiyus	CAS 254914	Skull	0.01936437	70	290	20.3	0.200103	0.5 mm Cu	1000	3	
Cordylus namakuiyus	CAS254914	Skeleton	0.13735179	120	150	18	0.333096	none	1000	3	
Cordylus namakuiyus	CAS 256529	Skull	0.01965777	80	200	16	0.200098	none	2300	3	
Cordylus namakuiyus	CAS 256529	Skeleton	0.0303892	140	200	28	0.333096	none	1500	3	
Cordylus namakuiyus	CAS 256530	Skull	0.01279052	80	150	12	0.200098	none	2200	3	
Cordylus namakuiyus	CAS 256530	Skeleton	0.01678024	100	200	20	1	0.1 mm Cu	1500	6	
Cordylus namakuiyus	CAS256531	Skull	0.00548933	80	200	16	0.500093	none	2200	3	
Cordylus namakuiyus	CAS256531	Skeleton	0.01564622	80	150	12	0.200098	none	1200	3	
Cordylus namakuiyus	PEM R18005	Skull	0.00359041	80	200	16	0.333096	none	2200	3	
Cordylus namakuiyus	PEM R18005	Skeleton	0.00448129	80	200	16	0.333096	none	2200	3	
Cordylus machadoi	PEM R18006	Skull	0.03708717	130	150	19.5	0.332453	none	1000	3	
Cordylus machadoi	PEM R18006	Skeleton	0.05977014	130	150	19.5	0.332453	none	1000	3	
Cordylus machadoi	PEM R18009	Skull	0.05188988	180	90	16.2	0.333	0.1 mm Cu	1250	3	
Cordylus machadoi	PEM R18009	Skeleton	0.08428062	160	28	4.48	0.333	none	1900	5	
Cordylus machadoi	PEM R19782	Skeleton	0.08428072	160	190	30.4	0.333	none	1900	5	
Cordylus machadoi	PEM R19784	Skeleton	0.06243877	155	195	30.225	0.333	0.5 mm Cu	1600	3	

MARQUES *ET AL.*